ORIGINAL RESEARCH

Expression of Mir-489-3p as an Effective Marker of Poor Prognosis in Patients with Non-small-cell Lung Carcinoma

Kang Zheng, MD; Jian Zheng, MD; Guanhua Liu, MD; Zhilong Li, MD

ABSTRACT

Context • Lung carcinoma accounts for the majority of cancer deaths, and its 5-year survival rate isn't optimistic. Remarkable progress has been made in recent decades toward understanding the biological behavior of non-small-cell lung carcinoma (NSCLC) and creating targeted molecular therapies for diagnosis and treatment. However, little literature is available on the topic, and the clinical significance and application of miR-489-3p for NSCLC can't yet be determined.

Objective • The study intended to determine if miR-489-3p can predict prognosis for patients with NSCLC.

Design • The research team designed a prospective study to examine in depth and analyze the molecular science of NSCLC tumors in a clinical setting.

Setting • The study took place in the Department of the Special Ward at the Shanxi Provincial Cancer Hospital in Taiyuan, Shanxi, China.

Participants • Participants were 116 patients with NSCLC at the hospital and 87 healthy people.

Outcome Measures • A type of microRNA (miRNA), MiR-489-3p, was detected using nano-polymerase chain reaction (PCR). The diagnostic value of miR-489-3p for lung carcinoma and its predictive value for death from the disease were analyzed using a receiver operating characteristic (ROC) curve, and the three-year prognosis for patients was examined. Human NSCLC cell lines and normal, human, lung epithelial cells were obtained, and miR-489-3p was detected to assess the biological effects on lung-cancer cells.

Results • MiR-489-3p has low expression in lung-cancer tissues, which indicates its good predictive value for prognosis for and death of lung-cancer patients. The activity of tumor cells increased after the inhibition of miR-489-3p.

Conclusions • A low level of miR-489-3p indicates a poor prognosis for patients with NSCLC. A deeper understanding of the mechanism of miR-489-3p in lung carcinoma may be the key to the earlier diagnosis and treatment of lung carcinoma. (*Altern Ther Health Med.* 2022;28(7):104-110).

Kang Zheng, MD, Physician; **Guanhua Liu,** MD, Physician; **Zhilong Li,** MD, Physician; Department of Special Ward. Shanxi Province Cancer Hospital/ Shanxi Hospital Affiliated to Cancer Hospital, Chinese Academy of Medical Sciences/ Cancer Hospital Affiliated to Shanxi Medical University, Taiyuan, Shanxi, China. **Jian Zheng**, MD, Physician, Department of Cardiopulmonary Function Examination, Shanxi Provincial Cancer Hospital, Taiyuan, Shanxi, China.

Corresponding author: Jian Zheng, MD
E-mail: zhengjian03517621@163.com

As the most fatal type of cancer, carcinoma of the lung is extremely detrimental, and non-small-cell lung carcinoma (NSCLC) is the typically observed tumor type.[1] NSCLC can be divided into three subgroups: lung adenocarcinoma, lung squamous-cell carcinoma, and large-cell carcinoma.[2,3] Most patients are found to be at the middle stage of the cancer's development upon diagnosis, which easily leads to a poor prognosis.[4]

According to Villalobos and Wistuba, 1.8-million people are diagnosed with lung cancer every year all over the world; nearly 1.6 million people die of the disease annually; and the five-year survival rate isn't optimistic.[5]

Smoking, air pollution, and occupational exposure are considered to be the main risk factors for lung carcinoma.[6,7] Especially in developing countries, the development of

industry and the gradual expansion of smoking groups have led to a significant upward trend in the incidence of lung cancer, and the disease also shows a trend toward greater incidence in younger people.[8,9]

Radical surgery is the main treatment at present, combined with radiotherapy and chemotherapy; those treatments, however, have many adverse reactions, some patients still have a risk of recurrence or metastasis, and the resulting prognosis is poor, with a low survival rate.[10,11] Also, the disease's etiology isn't completely clear.[12] Finding effective markers for a poor prognosis is of great significance for limiting the progression of NSCLC.

Remarkable progress has been made in recent decades toward understanding the biological behavior of NSCLC and creating targeted molecular therapies for diagnosis and treatment,[13] but the diagnosis and prognosis of patients remain unsatisfactory.[14]

As a result of in-depth studies of clinical molecular science, microRNA's (miRNA's) applications for and value in treatment of tumor diseases have attracted attention.[15] Ma has pointed out that miRNA plays an important role in tumorigenesis by regulating the cell cycle, metastasis, angiogenesis, metabolism, and apoptosis.[16] Zealy et al found that miRNA plays a role in tumor inhibition and carcinogenesis and can function as a diagnostic and prognostic biomarker in lung carcinoma.[17]

Two studies found that a decrease in the expression level of MiR-489-3p, a kind of miRNA, can cause the proliferation and invasion of tumor cells and the occurrence of tumors, such as glioma and melanoma.[18,19] In addition, Dao et al found that the expression of miR-489-3p had decreased in the serum of patients with lung cancer.[20]

Similarly, Sun et al found that miR-489-3p can also be used as a marker of poor prognosis of bladder carcinoma, which further showed that miR-489-3p might have a very high potential for application in treatment of NSCLC and even in other tumor diseases in the future [21] Kuppass has also confirmed the application value of miR-489-3p in determining tumor progression, further suggesting that miR-489-3p might be a marker for NSCLC.[22]

However, little literature is available on the topic, and the clinical significance and application of miR-489-3p for NSCLC can't yet be determined. Therefore, the current study intended to determine if miR-489-3p can predict the prognosis for patients with NSCLC.

METHODS

Participants

The research team designed a prospective study to examine in depth and analyze the molecular science of NSCLC tumors in a clinical setting. The study took place in the Department of the Special Ward at the Shanxi Provincial Cancer Hospital in Taiyuan, Shanxi, China. Potential participants were patients at the hospital between April 2015 and May 2017 who had NSCLC and 87 healthy people who came to our hospital for routine physical examination. Eligible subjects were selected as potential subjects according to the inclusion and exclusion criteria. Afterwards, the test team explained the purpose, method and possible results of the research to him, and asked him whether he was willing to participate in the experiment. If he agrees, he will be included in this study.

Potential participants who were patients were included if they had NSCLC that had been diagnosed early and that had been confirmed by pathology tests.

Potential participants who were patients were excluded if they: (1) had any other type of tumor, (2) had cardiovascular or cerebrovascular diseases, (3) had autoimmune diseases, (4) had organ failure, or (5) were pregnant.

Potential participants who were healthy were included if they: (1) willing to participate in this experiment, (2) 18-60 years old, (3) No history of major disease in the past.

Potential participants who were healthy were excluded if the results of the physical examination were abnormal, and it was found that some diseases may be present.

This study was approved by Ethics Committee of Shanxi Provincial Cancer Hospital. All patients signed an informed consent. The NSCLC participants also consented to a pathological examination.

Procedures

Groups. The participants with NSCLC were included in the observation group (OG), the intervention group, and the healthy people were included in the control group (CG).

Specimen collection. Four mL of venous blood was taken from fasting participants. To collect the upper-layer serum for later use, each sample was allowed to stand for 30 min before centrifugation for 10 min (400 × g). In addition, sections of cancer tissue and adjacent tissue sections surgically removed from NSCLC patients were obtained and stored in liquid nitrogen.

Mimics-miR-489-3p ininhibition-miR-489-3p, and NC-miR groups. The study compared various variables for the miR-489-3p mimic sequence (mimics-miR-489-3p group), the miR-489-3p inhibitor sequence (inhibition-miR-489-3p group), and the miR-489-3p negative control (NC-miR group): miR-489-3p expression and cell proliferation and migration rates. These cells were purchased from Thermo Fisher (Waltham, Massachusetts, USA). Cells were seeded in 96-well plates, and the above sequences were transfected into cells according to the instructions of Lipofectamine 2000 kit (Thermo Fisher, Waltham, Massachusetts, USA) to construct cells with abnormal expression of miR-489-3p.

Reagents. All cancer cells from the participants, cell lines, epithelial cells, and two groups were cultured in 5% CO_2, 37°C environment. Inoculated in RPMI-1640 + 10% FBS + 1% P/S medium (provided by ATCC), and then passaged after their confluency reached 80%. The study also used: (1) 3-(4,5-Dimethylthiazol-2-yl) (MTT) solution, (2) fetal bovine serum (FBS), (3) transfection reagents, (4) AnnexinV-FITC, (5) propidium iodide (PI), (6) phosphate buffer saline (PBS), (7) Trypsin and (8) Bax, Bcl-2 antibody.

Nano-polymerase chain reaction (PCR). The diagnostic role of miR-489-3p for NSCLC and its predictive value for NSCLC death were analyzed using a ROC curve, and the influence of miR-489-3p on the three-year prognosis of NSCLC patients was investigated.

The changes in the miR-489-3p in the OG group NSCLC were evaluated using a PCR. For the OG group, the study measured the miR-489-3p in the participants' serum, carcinoma tissues, and adjacent tissues. For the CG group, the study measured the miR-489-3p in the participants' serum.

Cell tissue from the tumor specimens was extracted using the nano-magnetic-bead method. The nano-magnetic beads are round spheres with a diameter of about 0.2 μm under the microscope, and they are densely arranged with small spaces between them. The cell morphology was observed using a transmission electron microscope (TEM) from KEYENCE (Osaka, Japan). The total RNA was reverse transcribed into complementary DNA (cDNA) and amplification was conducted according to the kit's instructions. The expression levels were calculated using the 2-ΔΔCt method: (1) ΔCT(test) = CT(target, test) – CT(ref, test), (2) ΔCT(calibrator) = CT(target, calibrator) – CT(ref, calibrator), (3) ΔΔCT = ΔCT(test) – ΔCT(calibrator).

Cell data and culture. The human NSCLC cell lines NCI-H1650, HCC827, and NCI-H1299 (BNCC100260, BNCC100261, BNCC100268) and human, normal lung epithelial cells CYP2A13 (BNCC101953) were obtained from Bena Biotechnology, a subsidiary company of ATCC (Baltimore, Maryland, USA). human non-small cell lung cancer cells (NCI-H1650), human non-small cell lung cancer cells (HCC827), human large cell lung cancer cells (NCI-H1299), and human normal lung epithelial cells (CYP2A13) were cultured in the corresponding media. Mir-489-3p cell proliferation was measured for these cell lines.

Cell transfection. Cells were seeded in 96-well plates, and the above sequences were transfected into cells according to the instructions of Lipofectamine 2000 kit (Thermo Fisher, Waltham, Massachusetts, USA) to construct cells with abnormal expression of miR-489-3p. Inhibition-miR-489-3p, mimics-miR-489-3p, and NC-miR were transfected into the NSCLC cell lines, and the experiment was continued after the transfection was successful. The miR-489-3p levels in the cell lines and in the two groups were measured.

Cell proliferation. The transfected cells were inoculated into 96-well plates and cultured for 24h. Then 20 μL of MTT solution (5 μg/ml) was added to each well of a microwell plate every 24 h, and the cultures were put into an incubator. After 4 hours: (1) the 96-well plate was taken out of the incubator; (2) the supernatant was discarded from each well; (3) 200 μLs of DMSO were added; and (4) the 490-nm microplate reader (Beideng TECAN F50, Nanjing, Jiangsu, China) was used for detection.

Cell invasion. The upper and lower compartments of the Transwell chamber were added with GC cells at the logarithmic phase (1×106/mL) and FBS, respectively, and then treated with 24 h incubation, and the remaining cells were stained and observed using a microscope.

Apoptosis. Transfected cells were: (1) digested with 0.25% trypsin, (2) rinsed with PBS, (3) added to 100 μL of binding buffer, (4) prepared into suspension, (5) added to AnnexinV-FITC and PI in turn, and (5) placed in the dark for 15 min. Afterward, 300 μL of buffer was added, and apoptosis was measured using flow cytometry.

Protein detection. The transfected cells were lysed. A sodium dodecyl sulfate–polyacrylamide gel electrophoresis (SDS-PAGE) gel was prepared, and the protein in the gel was transferred to a polyvinylidene fluoride (PVDF) membrane (Abcam, Cambridge, Cambridgeshire, UK) after protein electrophoresis. The primary antibody, at 1:1000, was cultivated at 4°C overnight. After washing the membrane with PBS, the secondary antibody, at 1:10 000, was cultivated for one h. Enhanced chemiluminescent (ECL) chemiluminescence solution (Biosharp, China) was applied for development, and the gray value of the target protein was measured using Image J software (National Institutes of Health, Bethesda, Maryland, USA).

Outcome Measures

MiR-489-3p expression. The total RNA was reverse transcribed into cDNA, amplification was carried out according to the kit instructions, and the expression levels were calculated using the 2-ΔΔCt method. If miR-489-3p in the observation group was higher than that in the control group, it indicated that miR-489-3p was highly expressed in NSCLC, and vice versa.

Occurrence of and prediction of death from NSCLC. An ROC analysis was performed on serum levels of miR-489-3p in both groups to assess the sensitivity and specificity of miR-489-3p in predicting the occurrence of NSCLC and death from NSCLC. Sensitivity: The percentage of patients who are actually diseased and correctly judged to be diseased according to the criteria of this diagnostic test. It reflects the ability of a diagnostic test to find patients. Specificity: The percentage of patients who are actually disease-free and correctly identified as disease-free by diagnostic tests. It reflects the ability of a diagnostic test to identify non-patients. Youden index: Also known as the correct index, it is a method to evaluate the authenticity of the screening test. The larger the index, the better the effect of the screening test and the greater the authenticity. Cutoff: the critical value, if the critical value is exceeded, the occurrence of the disease is considered. AUC: Area under the ROC curve. The closer the AUC is to 1.0, the higher the authenticity of the detection method; when it is equal to 0.5, the authenticity is the lowest and has no application value.

Levels of miR-489-3p and prognosis. The study measured the ability of miR-489-3p to predict death within three years. According to a cut-off value for miR-489-3, the participants in the OG group with a cut-off value of >0.468 for miR-489-3 were assigned to a high miR-489-3p group (n = 72), and those with a cut-off value of ≤0.468 were assigned to a low miR-489-3p group (n = 44); 0 = low survival rate and 100 = high survival rate.

Cell proliferation and cell migration: The NCI-H1650 and HCC827 cell lines, which had the lowest miR-489-3p expression, were selected for biological detection. In-vitro experiments were conducted to analyze the mechanism of miR-489-3p in the disease, and the expression of miR-489-3p in all NSCLC cell lines was detected. The higher the detection result, the stronger the cell invasion and migration ability.

Apoptosis and Apoptotic Protein. Apoptosis was measured using flow cytometry, and the expressions of apoptosis-related proteins Bax and BCL-2 were detected by Western blotting. The higher the apoptosis rate and Bax, the stronger the apoptosis ability. The higher the Bcl-2, the stronger the anti-apoptotic ability of the cells.

Statistical Analysis

SPSS24.0 software (Yuchuang Network, Shanghai, China was applied for data testing, and Graphpad8 (GraphPad Software, San Diego, California, USA) was used for visualization of the graphs. A *t* test was applied for the measurement of data comparisons. Single-factor analysis of variance (ANOVA) and least significant difference (LSD) back-testing were applied for multigroup comparisons. The diagnostic function was assessed using an ROC curve. Survival rate was calculated using the Kaplan-Meier method. A $P < .05$ indicates statistical significance.

RESULTS

The study analyzed the data of the 116 participants with NSCLC in the OG group and the 87 healthy participants in the CG group.

MiR-489-3p Levels

Figure 1A shows the morphology of magnetic nanobeads used to extract total RNA in this study. that was used in the nano-PCR, which showed that the miR-489-3p in the OG group was lower than that in the CG group, with $P < .05$ (Figure 1B). Further detection of miR-489-3p expression levels in cancer tissues and adjacent tissues also found that the expression of miR-489-3p in cancer tissues was lower than that in adjacent tissues of the OG group, with $P < .05$ (Figure 1C). Therefore, miR-489-3p was underexpressed in participants with NSCLC.

Diagnostic Role of MiR-489-3p

To assess the diagnostic value of miR-489-3p for NSCLC, an ROC analysis on the serum levels of miR-489-3p was performed for both groups. The ROC showed that the diagnostic sensitivity and specificity of miR-489-3p for NSCLC, when the AUC was 0.780 and the cut-off value was >1.319, were 52.87% and 91.38%, respectively, with $P < .001$ (Figure 2 and Table 1). This finding indicates that miR-489-3p has excellent specificity for the diagnosis of NSCLC.

Predictive Role for Death From NSCLC

The prognostic significance of OG group' miR-489-3p in NSCLC was further analyzed, and 100% of enrolled

Figure 1. Mir-489-3p Expression.Figure 1A shows the morphology of magnetic nanobeads used to extract total RNA in this study; Figure 1B shows the miR-489-3p in the OG and CG; Figure 1C shows the miR-489-3p in cancer tissues and adjacent tissues.

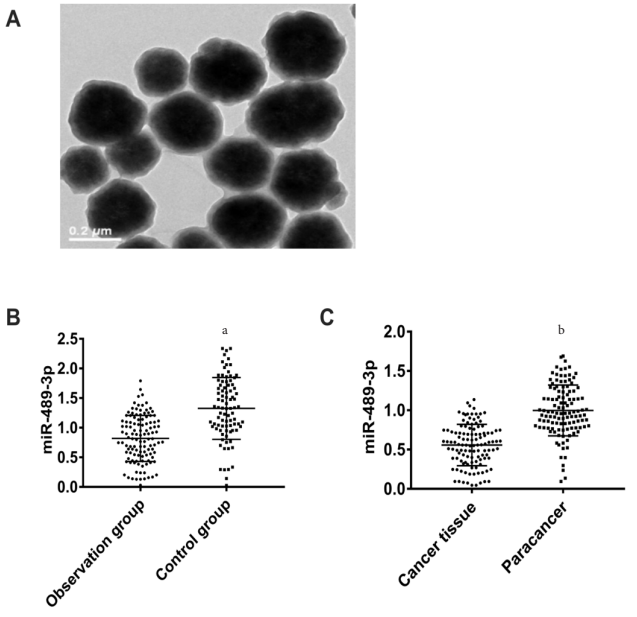

[a]$P < .05$, shows that the OG group's miR-489-3p expression was significantly lower than that of the CG group

[b]$P < .05$, shows that miR-489-3p expression in cancer tissues was lower than that in the adjacent tissues of the OG group

Abbreviations: CG**,** control group**;** Mir-489-3p, microRNA-489-3p; OG, observation group (intervention group); polymerase chain reaction (PCR).

Figure 2. ROC Curve of Mir-489-3p for Predicting the Occurrence of NSCLC. For the diagnostic sensitivity and specificity of miR-489-3p in predicting the occurrence of NSCLC, $P < .001$ showed statistical significance.

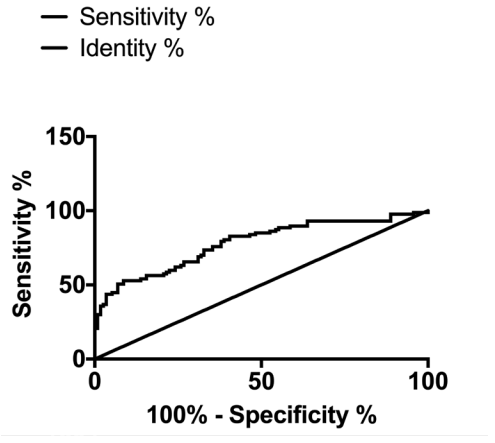

Abbreviations: Mir-489-3p, microRNA-489-3p; NSCLC, non-small-cell lung cancer; ROC, receiver operating characteristic

Table 1. Diagnostic Role of Mir-489-3p in NSCLC

	Mir-489-3p
AUC	0.780
Standard Error	0.033
95% CI	0.714~0.845
Cut-off	>1.319
Sensitivity, %	52.87
Specificity, %	91.38
Youden index, %	44.25
P Value	<.001[a]

[a]$P < .001$, showing that Mir-489-3p's ability to predict the occurrence of NSCLC was statistically significant.

Abbreviations: AUC, area under curve; CI, confidence interval; Mir-489-3p, microRNA-489-3p; NSCLC, non-small-cell lung cancer

Table 2. Diagnostic Role of Mir-489-3p in the Prediction of Death From NSCLC

	miR-489-3p
AUC	0.843
Standard Error	0.055
95% CI	0.735~0.951
Cut-off	>0.468
Sensitivity, %	68.27
Specificity, %	91.67
Youden index, %	59.94
P Value	<.001[a]

[a]$P < .001$, showing that Mir-489-3p's ability to predict death from NSCLC was statistically significant

Abbreviations: AUC, area under curve; Mir-489-3p, microRNA-489-3p; NSCLC, non-small-cell lung cancer.

Figure 3. ROC Curve of Mir-489-3p for Predicting Death From NSCLC. For prediction of death from NSCLC using miR-489-3p, $P < .001$ showed statistical significance.

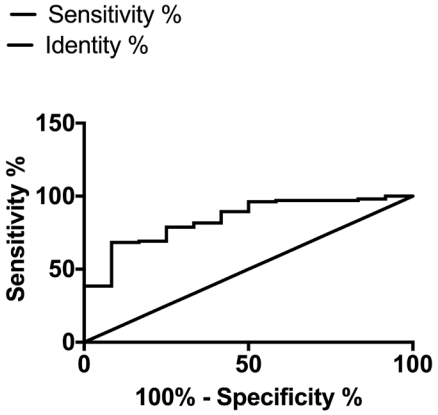

Abbreviations: Mir-489-3p, microRNA-489-3p; NSCLC, non-small-cell lung cancer; ROC, receiver operating characteristic.

Figure 4. Role of Mir-489-3p in the Prognosis of Participants With NSCLC. For stating the ability of miR-489-3p to prognostically predict an increased risk of death for NSCLC patients, $P < .028$ showed statistical significance.

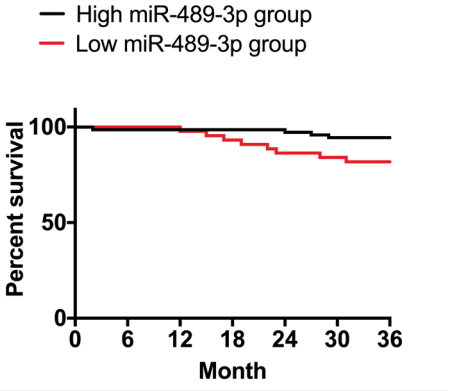

Abbreviations: Mir-489-3p, microRNA-489-3p; NSCLC, non-small-cell lung cancer.

participants were successfully followed up. Data for the OG group were statistically analyzed and divided into a death group, 12 participants, and a survival group, 104 participants. The predictive role of miR-489-3p for death from NSCLC was analyzed using an ROC curve. The data showed that the sensitivity and specificity of miR-489-3p for death from NSCLC, when the area under curve (AUC) was 0.843 and the cut-off value was 0.468, were 68.27% and 91.67%, respectively, with $P < .001$ (Figure 3 and Table 2).

MiR-489-3p and Prognosis

In a comparison of their prognoses and survival rates, prognosis was found to be better in the high miR-489-3p group compared to that in the low miR-489-3p group, with $P < .028$ (Figure 4) group, suggesting that a decrease in the miR-489-3p level can prognostically predict an increased risk of death for NSCLC patients.

Proliferation and Invasion of NSCLC

The nano-PCR found that the miR-489-3p in the NCI-H1650, HCC827, and NCI-H1299 cell lines decreased significantly, with $P < .05$ (Figure 5A), which is consistent with the expression of miR-489-3p in NSCLC.

After transfection of the cells with either mimics-miR-489-3, the intervention group, or inhibition-miR-489-3p, the proliferation and invasion of cells transfected with mimics-miR-489-3p were significantly lower than that of cells in the NC-miR group, the negative control group, and that of cells transfected with inhibition-miR-489-3p, with $P < .05$ (Figure 5B, 5C, and 5D). These results suggest that increasing miR-489-3p expression can inhibit the activity of NSCLC cells.

Apoptosis and Apoptotic Protein

The apoptosis rate in the miR-489-3p-mimics group, the intervention group, was significantly higher than that of the

Figure 5. Role of Mir-489-3p on Cell Activity. Figure 5A shows miR-489-3p in the NSCLC cell lines; Figure 5B shows the proliferation in the NCI-H1650 cell line; Figure 5C shows the proliferation in the HCC827 cell lines; and Figure 5D shows cell invasion in both cell lines.

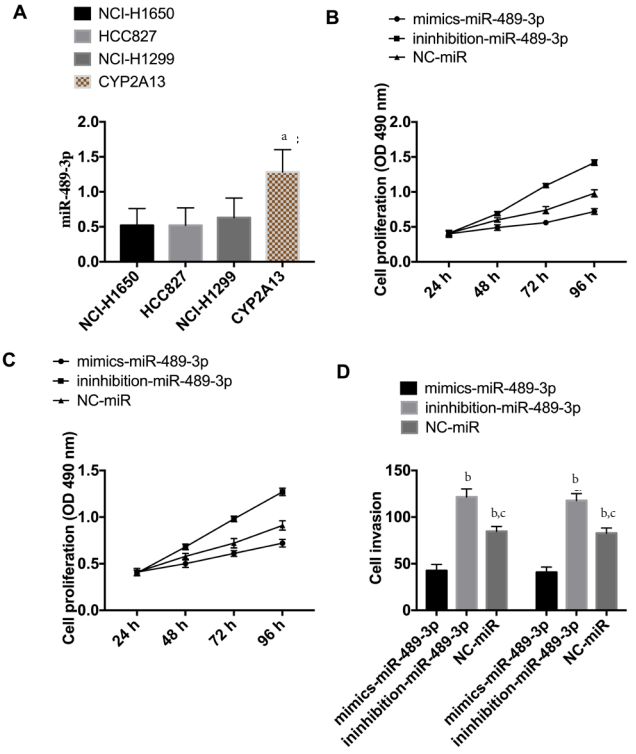

[a]$P < .05$ shows that the cell proliferation in the CYP2A13 cells was significantly higher than that in the three NSCLC cell lines.

[b]$P < .05$ in Figure 5B, C shows that the cell proliferation in the ininhibition-miR-489-3p group cell line was significantly higher than that in miR-489-3p-mimics group and NC-miR group.

[c]$P < .05$ in Figure 5B, C shows that the cell proliferation in the NC-miR group cell line was significantly higher than that in miR-489-3p-mimics group cell lines.

Abbreviations: CYP2A13, human normal lung epithelial cells; HCC827, human NSCLC cell line; mir-489-3p, microRNA-489-3p; mimics-miR-489-3p group, the intervention group; NCI-H1299, human NSCLC cell line; NCI-H1650, human NSCLC cell line; NC-miR, negative control group; NSCLC, human non-small-cell lung cancer

Figure 6. Role of Mir-489-3p on Apoptosis for the NCI-H1650 and HCC827 cell lines. Figure 6A shows the apoptosis; Figure 6B shows the apoptotic protein; Figure 6C shows the flow cytometry of the NCI-H1650 cell line; Figure 6D shows flow cytometry of the HCC827 cell line; and Figure 6E shows imprinting map of the apoptotic protein.

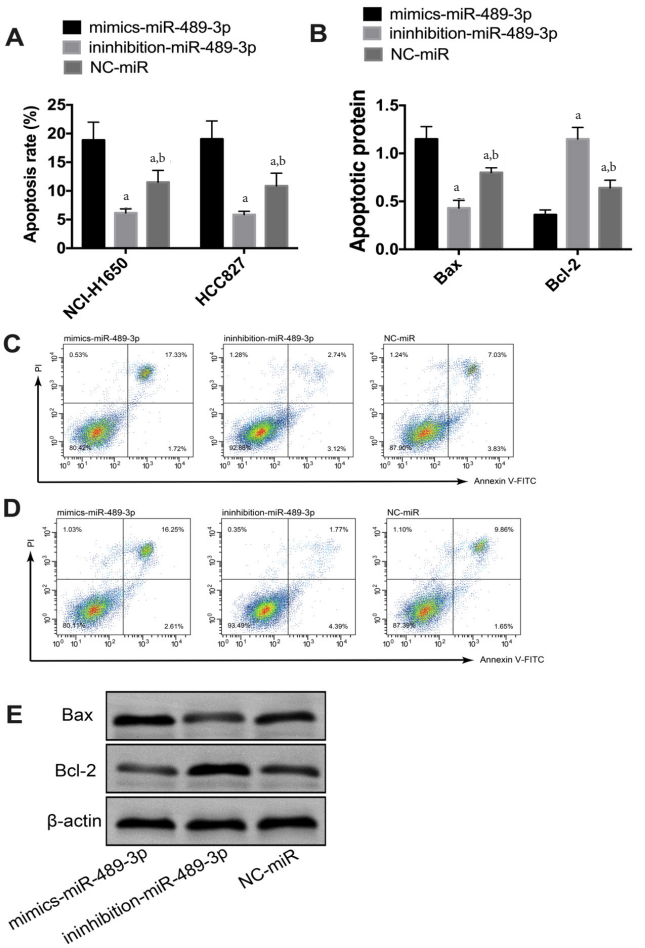

[a]$P < .05$ shows that the apoptosis rate of inhibition-miR-489-3p group was lower than that of miR-489-3p-mimics group and NC-miR group.

[b]$P < .05$ shows that the apoptosis rate of NC-miR group was lower than that of miR-489-3p-mimics group.

Abbreviations: B-actin, beta actin; Bax, Bax, BCL2 associated X; Bcl-2, Bcl-2, B-cell lymphoma-2; mimics-miR-489-3p group, OG (intervention) group; Mir-489-3p, microRNA-489-3p; NCI-H1650, human NSCLC cell line; HCC827, human NSCLC cell line; NC-miR, negative control group; NSCLC, human non-small-cell lung cancer

ininhibition-miR-489-3p group and the NC-miR group, the negative control group, with $P < .05$ (Figures 6A, 6C, and 6D). In addition, in the miR-489-3p-mimics group, the Bax pro-apoptotic protein increased and the Bcl-2 anti-apoptotic protein decreased, with $P < .05$ (Figures 6B and 6E).

DISCUSSION

The current study explored the potentially effective markers for poor prognosis in NSCLC patients and provided methods for future clinical diagnosis and treatment. The research showed that miR-489-3p was low in the NSCLC participants, suggesting that miR-489-3p levels correlate with

the progression of NSCLC. Bai et al[23] study, which explored miR-489-3p in prostate carcinoma, supports the current study's findings.

In the current study, the ROC curve showed that the sensitivity and specificity of miR-489-3p in the diagnosis of NSCLC were 52.87% and 91.38%, suggesting that miR-489-3p may be used for NSCLC screening in the future. The data indicated that miR-489-3p had a higher specificity, providing more clinical diagnostic advantages than traditional tumor markers and allowing disease treatment to occur more rapidly, with an improved prognosis. We believe that the clinical application of miR-489-3p in the future can effectively improve the early diagnosis rate of NSCLC, thereby assisting the clinical treatment of patients in a more timely and accurate manner and improving the prognosis of patients.

The current research team also followed up with the participants to further test miR-489-3p in NSCLC and found that when the AUC was 0.843 and the cut-off value was 0.468, the sensitivity and specificity of miR-489-3p in predicting death within three years of prognosis were 68.27% and 91.67%, respectively. Similar to Sun et al's findings in bladder cancer,[24] A lower miR-489-3p indicates a greater risk of death, and highly expressed miR-489-3p can be used as a marker for poor prognosis as a clinical reference, which indicates that miR-489-3p may have very high potential in NSCLC and in other tumor diseases in the future. This can also effectively solve the current situation of the lack of clinical evaluation methods for the prognosis of tumor patients. We speculate that in the future, real-time detection of miR-489-3p expression during the treatment of NSCLC patients can assist in clinical assessment of the patient's condition changes and formulate the best treatment plan. At the same time, since the detection of miR-489-3p is also more objective compared with the results of imaging examination, it will also reduce the incidence of misdiagnosis. It can be seen that miR-489-3p is of great significance for the clinical diagnosis and treatment of NSCLC in the future, which is also an important reason for our continued in-depth analysis.

The current study had some limitations. First, the data from patients with other types of lung carcinoma haven't been explored in the current study, so the research team couldn't make conclusions about the specific effects of miR-489-3p in different types of lung carcinoma. Second, the experimental period was short, and the effects of miR-489-3p on long-term prognosis wasn't clear. The research team intends to perform a more detailed exploration in the future to obtain the best experimental results.

CONCLUSIONS

A low level of miR-489-3p indicates a poor prognosis for patients with NSCLC. A deeper understanding of the mechanism of miR-489-3p in lung carcinoma may be the key to the earlier diagnosis and treatment of lung carcinoma.

AUTHOR CONTRIBUTIONS

Kang Zheng and Jian Zheng made Contributed equally to this work

AUTHORS' DISCLOSURE STATEMENT

The research team has no conflicts of interest related to the study.

REFERENCES

1. Hirsch FR, Scagliotti GV, Mulshine JL, et al. Lung cancer: current therapies and new targeted treatments. *Lancet*. 2017;389(10066):299-311. doi:10.1016/S0140-6736(16)30958-8
2. Duma N, Santana-Davila R, Molina JR. Non-small-cell lung cancer: Epidemiology, screening, diagnosis, and treatment. *Mayo Clin Proc*. 2019;94(8):1623-1640. doi:10.1016/j.mayocp.2019.01.013
3. Ettinger DS, Wood DE, Aisner DL, et al. Non-small-cell lung cancer, version 5.2017, NCCN Clinical Practice Guidelines in Oncology. *J Natl Compr Canc Netw*. 2017;15(4):504-535. doi:10.6004/jnccn.2017.0050
4. Vecchiarelli S, Bennati C. Oncogene addicted non-small-cell lung cancer: current standard and hot topics. *Future Oncol*. 2018;14(13s):3-17. doi:10.2217/fon-2018-0095
5. Villalobos P, Wistuba II. Lung cancer biomarkers. *Hematol Oncol Clin North Am*. 2017;31(1):13-29.doi:10.1016/j.hoc.2016.08.006
6. Nasim F, Sabath BF, Eapen GA. Lung Cancer. *Med Clin North Am*. 2019;103(3):463-473. doi:10.1016/j.mcna.2018.12.006
7. Bialous SA, Sarna L. Lung cancer and tobacco: what is new? *Nurs Clin North Am*. 2017;52(1):53-63. doi:10.1016/j.cnur.2016.10.003
8. Romaszko AM, Doboszyńska A. Multiple primary lung cancer: A literature review. *Adv Clin Exp Med*. 2018;27(5):725-730. doi:10.17219/acem/68631
9. De Sousa V, Carvalho L. Heterogeneity in Lung Cancer. *Pathobiology: journal of Immunopathology*. *Mol Cell Biol*. 2018;85(1-2):96-107.
10. Duruisseaux M, Esteller M. Lung cancer epigenetics: from knowledge to applications. *Semin Cancer Biol*. 2018;51:116-128. doi:10.1016/j.semcancer.2017.09.005
11. Chassagnon G, Bennani S, Revel MP. [New TNM classification of non-small cell lung cancer]. *Rev Pneumol Clin*. 2017;73(1):34-39. doi:10.1016/j.pneumo.2016.12.006
12. Mott TF. Lung Cancer: management. *FP Essent*. 2018;464:27-30.
13. Jonna S, Subramaniam DS. Molecular diagnostics and targeted therapies in non-small cell lung cancer (NSCLC): an update. *Discov Med*. 2019;27(148):167-170.
14. Watanabe SI, Nakagawa K, Suzuki K, et al; Lung Cancer Surgical Study Group (LCSSG) of the Japan Clinical Oncology Group (JCOG). Neoadjuvant and adjuvant therapy for Stage III non-small cell lung cancer. *Jpn J Clin Oncol*. 2017;47(12):1112-1118. doi:10.1093/jjco/hyx147
15. Lu TX, Rothenberg ME. MicroRNA. *J Allergy Clin Immunol*. 2018;141(4):1202-1207. doi:10.1016/j.jaci.2017.08.034
16. Ma Y. The challenge of microRNA as a biomarker of epilepsy. *Curr Neuropharmacol*. 2018;16(1):37-42.
17. Zealy RW, Wrenn SP, Davila S, Min KW, Yoon JH. microRNA-binding proteins: specificity and function. *Wiley Interdiscip Rev RNA*. 2017;8(5):1-8. doi:10.1002/wrna.1414
18. Yang X, Zhu X, Yan Z, et al. miR-489-3p/SIX1 axis regulates melanoma proliferation and glycolytic potential. *Mol Ther Oncolytics*. 2019;16:30-40. doi:10.1016/j.omto.2019.11.001
19. Zhang L, Wang Q, Wang F, et al. LncRNA LINC01446 promotes glioblastoma progression by modulating miR-489-3p/TPT1 axis. *Biochem Biophys Res Commun*. 2018;503(3):1484-1490. doi:10.1016/j.bbrc.2018.07.067
20. Dao R, Wudu M, Hui L, Jiang J, Xu Y, Ren H, Qiu, X. Knockdown of lncRNA MIR503HG suppresses proliferation and promotes apoptosis of non-small-cell lung cancer cells by regulating miR-489-3p and miR-625-5p. *Pathology, Research, and Practice*. 2020; 216(3):152823(1)-152823(10). doi:10.1016/j.prp.2020.152823
21. Chen L, Chen L, Qin Z, et al. Upregulation of miR-489-3p and miR-630 inhibits oxaliplatin uptake in renal cell carcinoma by targeting OCT2. *Acta Pharm Sin B*. 2019;9(5):1008-1020. doi:10.1016/j.apsb.2019.01.002
22. Kuppa SS, Jia W, Liu S, et al. Autotaxin exacerbates tumor progression by enhancing MEK1 and overriding the function of miR-489-3p. *Cancer Lett*. 2018;432:84-92. doi:10.1016/j.canlet.2018.05.037
23. Bai P, Li W, Wan Z, et al. Mir-489-3p inhibits prostate cancer progression by targeting DLX1. *Cancer Manag Res*. 2020;12:2719-2729. doi:10.2147/CMAR.S239796
24. Sun D, Li T, Xin H, An J, Yang J, Lin J, Meng X, Wang B, Ozaki T, Yu M, Zhu, Y. Mir-489-3p inhibits proliferation and migration of bladder cancer cells through downregulation of histone deacetylase 2. *Oncology Letters*. 2020; 20(4:8(1)-8(12).